

# Strong Halogen Bonding and Electron Transfer between Halide Anions and Halogen-Containing Imides and Saccharines

An Honors Thesis (Hon 499)

By Spencer Deats

Thesis Advisor- Dr. Sergiy Rosokha

Ball State University

Muncie Indiana

September 2019

Expected Date of Graduation

May 2020

## Abstract

Halogen bonding represents an interesting form of intermolecular attraction that has recently been recognized as a useful tool in preparation of certain materials and molecular recognition in some chemical and biochemical systems. Halogen bonding is formed between a halogen and an electron rich species on another molecule. Strong halogen bonding specifically was studied in this experiment. The strong halogen bonding's thermodynamic properties, such as equilibrium constants and extinction coefficients, are currently understudied and not well known. Knowledge of these numbers will improve their ability to be used for preparation of materials and their use in molecular recognition in other fields of study. Using Uv-Vis spectroscopy, a wide variety of halogen bond donors and halogen bond acceptors were studied. The acceptors studied were Bromide, Chloride and Iodide anions. And the halogen bond donors studied were halogen containing imides and saccharines. This study found that strong halogen bonding is between 3-1000 times stronger than typical halogen bonding from determining the equilibrium constants and extinction coefficients of various saccharines and imide systems.

## Acknowledgments

This research was started in the spring of 2018, during which time it was funded by the National Science Foundation (grant CHE1607746).

Also, a special thanks to my mentor on this project, Dr. Sergiy Rosokha, for allowing me to work in his lab and for his guidance throughout the research process.

I would also like to thank everyone in my lab group for being a part of this experience, especially Jessalyn Nicohlas for working as my partner on the early stages of the projects and John Brown for his collection of some data.

## Process Analysis Statement

I began working with Dr. Rosokha in January of 2018 at Ball State as a research assistant. His main research area is in physical organic chemistry, especially focusing on reactions and equilibriums. Immediately after I began working in his lab, he started me on the strong halogen bonding experiment.

My main task was to try and find the equilibrium constants and extinction coefficients of so-called strong halogen bonded complexes. The compounds that I was using were the bulky organic molecules of saccharine, succinimide and eventually phthalimide bonded to a halogen. This acted as the halogen bond donor and a halogen anion that was obtained through a halogen being attached to another large organic salt, usually tetrapropylammonium. I would make solutions from the compounds using acetonitrile as the solvent, then I would mix small amounts of the solutions and run them through a Uv-Vis spectrophotometer. The actual experiment was performed by holding the concentration of one solution constant and decreasing the concentration of the other solution and running the mixture of those two solutions, diluted up to a constant amount, through the Uv-Vis spectrophotometer.

The most difficult part of this experiment to perform was preventing the various solutions from becoming contaminated with the other solution I was working with at the time. What I mean by this is that since the concentrations were very small, I would need to be very careful that the glassware I was using was always clean, both before I started the experiment and during the experiment itself. In order to make sure that the glassware I was using was clean while performing the experiments, I would need to rinse out the old solution that was no longer used. This was done using the solvent for the solutions. I would rinse the glassware that was used to mix the two solutions, and then make sure it was dry before I could start to mix another solution.

Despite the care, it was still difficult to ensure that enough of the previous solution had been washed away so as to not impact the next mixture. If the old solution was allowed to mix with the newer one, then there would be no way to accurately measure the amount of donor or acceptor in the solution, thus making whatever data obtained from the measurement very inaccurate.

Research into this area is still new and not very fully explored so it was not always clear what some of the compounds should look like, and even after doing work on this project for nearly a year and a half, some of the results were still surprising. For instance, the phthalimide compounds ended up all being time dependent, which means that they could not be studied in the same way that the other compounds were. This was surprising as the only complexes that had been time dependent were just the ones that formed with Iodide as the bond donor. The structure of phthalimide looks very similar to that of saccharine, so we would expect that the complex formation to be similar to that of saccharine.

## Introduction

Halogen bonding is an intermolecular bond formed between a halogen and another electron rich species<sup>1</sup>. Halogens are found in Group VII of the Periodic Table and are known for being very reactive due to their nearly full electron shells. The bonding occurs due to non-covalent interactions formed by an area of positive potential of a covalently bonded halogen and a negative site<sup>1</sup>. The positive electrostatic region is labeled the  $\sigma$  hole<sup>2</sup>. These so called  $\sigma$  holes are what allows the areas of negative potential to bond to the areas of positive potential, thus creating an intermolecular bond between the halogen and the electron rich species<sup>2</sup>. While this form of bonding is quite similar to hydrogen bonding, the strong halogen bonding studied in this experiment is significantly stronger than the more well studied hydrogen bonding<sup>3</sup>. The bonding studied in this experiment had a halogen anion act as the halogen bond acceptor and the neutral halogen attached to a large organic molecule, such as a saccharine, act as the halogen bond donor. A model of a similar looking bonding is shown in Figure 1.

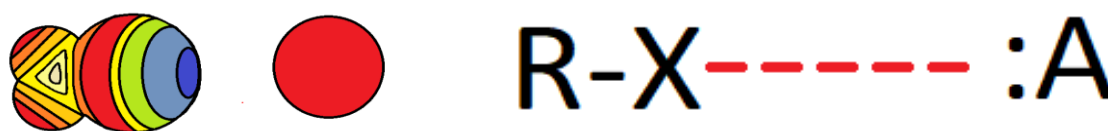


Figure 1. The image on the left shows a model of hydrogen bonding. The red sphere is an electron rich anion,  $I^-$ ,  $Br^-$ ,  $Cl^-$ , or  $F^-$ . The areas of positive electrical potential are shown in blue with areas of negative electrical potential shown in red. The figure on the right details the formula for the bonding, R is typically carbon or nitrogen and A is the electron rich anion.

Many different forms of this bonding were discovered throughout the 1800's to the 1900's but it was not recognized as halogen bonding until much later. It was also recently recognized as being overall the same kind of bonding. This prompted a surge of research into this kind of bonding and it was discovered to have useful properties in the fields of biochemical procedures and in

crystal engineering or material sciences<sup>4</sup>. In biochemical procedures, halogens are lipophobic so they are utilized in order to get through cell membranes, and in crystal engineering, the strength of the individual bonds can be carefully controlled via the kinds of halogens used to bond to one another. This allows for more careful control over the size of the crystals. In general, the bond strength of the halogen bonds is represented as  $I > Br > Cl > F$ . This was found through the work of Mulliken in the late 1960's and despite this work that earned a Nobel prize, not much research had been done into the thermodynamic properties of the bonding<sup>5</sup>.

The reason for this study was to determine some of the thermodynamic properties of the bonding while in solution. It was initially looked at because of some properties noted earlier in research. One of these properties is a shortening of the bond length between the two halogen species that are bonded. In most cases with weaker bonding, the bond length shortens by around 10-15%. But, in the case of the stronger halogen bonding the bond length shortens by nearly 25%. This leads to the theory that the bonding strength and equilibrium constant will be much larger than other similar forms of this bonding, but it has not been studied in the solution phase and the purpose was to determine the equilibrium constant and the overall bonding strength of this form of halogen bonding. This was done through the use of the N-halosubstituted imides and saccharine molecules when mixed with iodide, bromide and chloride anions. These anions were obtained by halogens attached to bulky organic salts, such as tetrapropylammonium dissolved in solution. The structures of the anions are shown in Figure 2 with X representing Chlorine, Bromine and Iodine for the various halogens utilized.

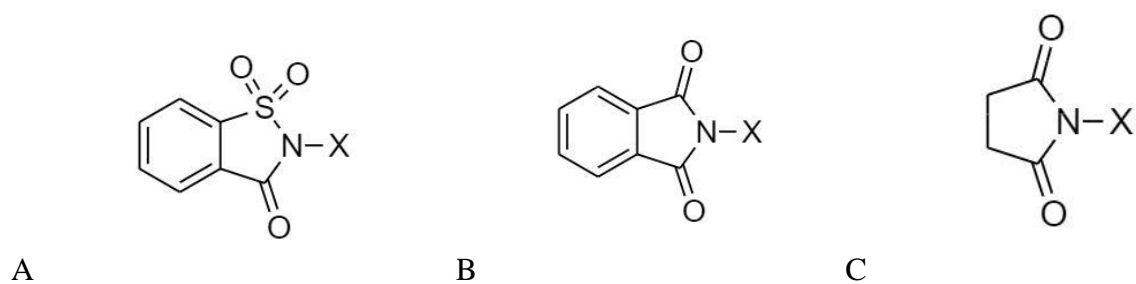


Figure 2: A) Chemical structure of halo-substituted saccharines. B) Chemical structure of halo-substituted Phthalimides. C) Chemical structure of halo-substituted succinimides. All) X=I, Br, Cl

## Experimental

The anions, obtained from salts, utilized were Tetrapropylammonium Iodide, Tetrapropylammonium Bromide, and Tetrapropylammonium Chloride, (TPAX). These anions were obtained from previous students work in recrystallization of these commercially available compounds. The halogen bond donors that were used were Bromosuccinimide, Chlorosuccinimide, Iodosuccinimide, (XSIM), Bromosaccharine, Chlorosaccharine, Iodosaccharine, (XSAC), Bromophthalimide, Chlorophthalimide, and Iodophthalimide, (XPIM). X represents Bromine, Chlorine or Iodine in both the donors and the acceptors. The halogen donors that were used were all commercially available and were purchased from Tokyo Chemical Industry Co.

In order to show that the bonding occurred, UV-Vis spectroscopy was utilized. They were studied by first creating solutions of the individual components and running portions of those solutions through a Uv-Vis spectrophotometer to determine what the individual components looked like. Then small amounts of the solutions were mixed and diluted up to 2 mL in acetonitrile and run through the Uv-Vis spectrophotometer in a 1 cm or 0.5mm cuvette. From



these solutions that were made, usually 0.5mL of the bond donor was taken with variable amounts of the bond acceptor. These amounts varied from 0.5mL and decreased to 0.05mL. The changes in absorbance between the individual components was noted and from there, a series was run with decreasing halogen bond acceptor concentration. From these new absorbance bands, the wavelength that produced the maximum absorbance was determined and the maximum absorbance was recorded for use in the determination of thermodynamic properties.

Experiments were performed with a halogen donor concentration range of  $4.24 \times 10^{-5}$  M in the experiments with BrSAC and TPABr to an upper concentration of  $7.5 \times 10^{-3}$  in the experiments with ClSIM and TPABr. The experiments with the halogen bond acceptor ranged from a low concentration of  $2.04 \times 10^{-3}$  in the experiment with ISIM and TPABr to an upper concentration of  $5.1 \times 10^{-2}$  in the experiments involving ClPIM and TPACl.

Extinction coefficients ( $\epsilon$ ) for halogen donors (XB), and halogen anions ( $X^-$ ) complexes and equilibrium constants of their formation, K were calculated via regression analysis of the dependence of the differential intensity of absorption (obtained by subtraction of absorption of components from the absorption of their mixtures) of solutions containing constant concentrations of and variable concentrations of halide anions:



$$Y = \epsilon l \left( \left( \frac{A+x+\frac{1}{K}}{2} \right) - \left( \frac{\left( \left( A+x+\frac{1}{K} \right)^2 - 4 \cdot A \cdot x \right)^{0.5}}{2} \right) \right) \quad (1).$$

Where y is the complex absorbance after baseline correction and subtraction of the individual components. A is the donor concentration and x is the acceptor concentration. This equation assumes a 1:1 complex stoichiometry.

In order to show where the complexes themselves absorbed, the individual components or species that were combined to form these complexes must have their absorbances subtracted from the complex data. This was done using excel spreadsheets. The concentration of the variable species was determined during each trial and then the ratio of that trial to the species alone was determined. The species alone was then multiplied by this ratio and then subtracted from the complex measurement via the excel subtraction function. This allows for just the complex to be viewed and was applied to all trials which had data that warranted further analysis.

## Results and Discussion

### Section I- Time Independent complexes

The BrSAC and TPABr complex is the complex that was studied the most out of any combination of individual components. In this complex it was noted that the ratio of donor to acceptor needed to be much more in favor of the acceptor. Before this complex, the data produced was not consistent as the components were not in a 1:1 ratio after they had reacted. It was through the work of another student in the lab, John Brown, that the complex was accurately recorded and used as a basis for what many of the future complexes should look like.

The complex of BrSAC and TPABr was studied as described in the experimental section and was run many times in order to confirm the thermodynamic numbers that were generated. The cleanest Uv-Vis measurements are shown in Figure 3. The BrSAC had a stock concentration of  $2.0 \times 10^{-4}$  M and the TPABr had a stock concentration of  $2.0 \times 10^{-4}$ . The BrSAC concentration in complex was held constant at  $5.0 \times 10^{-5}$  M and the TPABr concentration was decreased from  $5.0 \times 10^{-5}$  M to  $1.0 \times 10^{-5}$  M.

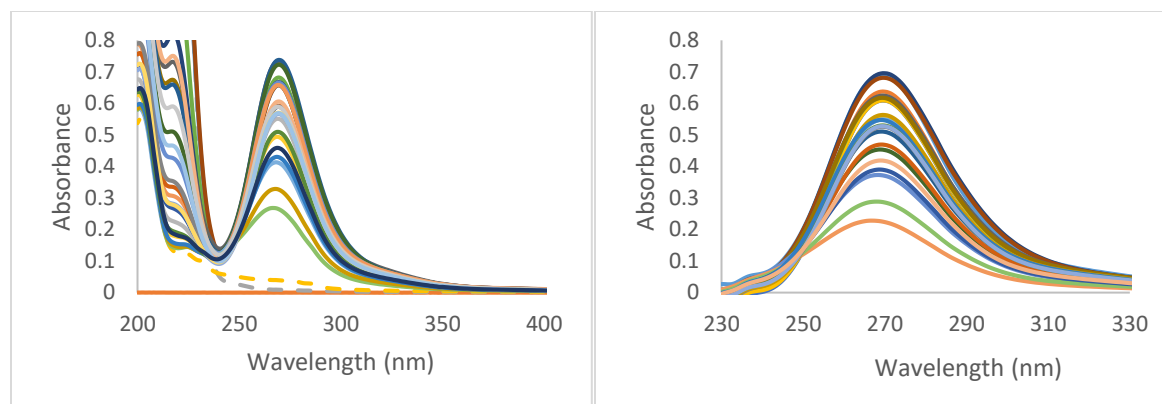


Figure 3: (Left) Uv-Vis spectra of BrSAC-TPABr with individual components as dashed lines, complex shown as solid lines. (Right) Excel graph showing spectra of BrSAC-TPABr with individual components subtracted out

This figure shows the difference in absorbance spectra before and after mixing. Before mixing, there is no peak, and after the two solutions are mixed there is a strong absorbance band peak at 270 nm that increases with increasing bromide concentration. This peak is indicative of the complex formation and is especially clear once the individual components are subtracted away. This difference in absorbance before and after mixing were used throughout the experiment in order to determine if a complex had formed. The wavelength that the peaks formed at were where the absorbance maxima were taken to be used in equation 1 when calculating  $K_{eq}$  and  $\epsilon$  values.

The next most studied combination was the complex of BrSIM and TPABr. This complex was another that ended up being a basis for what other complexes should look like but was less studied by other students in the lab. The complex of BrSIM and TPABr was studied in much the same way that BrSAC and TPABr was studied but the concentrations were as follows. The BrSIM had a stock concentration of  $1.1 \times 10^{-4}$  M and the TPABr had a stock concentration of  $2.9 \times 10^{-4}$ . The BrSIM concentration in complex was held constant at  $5.4 \times 10^{-5}$  M and TPABr's

concentration was changed from  $1.5 \times 10^{-5} \text{ M}$  to  $1.1 \times 10^{-5} \text{ M}$ . The spectra measurements of BrSIM and TPABr are shown in Figure 4 and the fitting function created using Origin and equation 1 is shown in Figure 5.

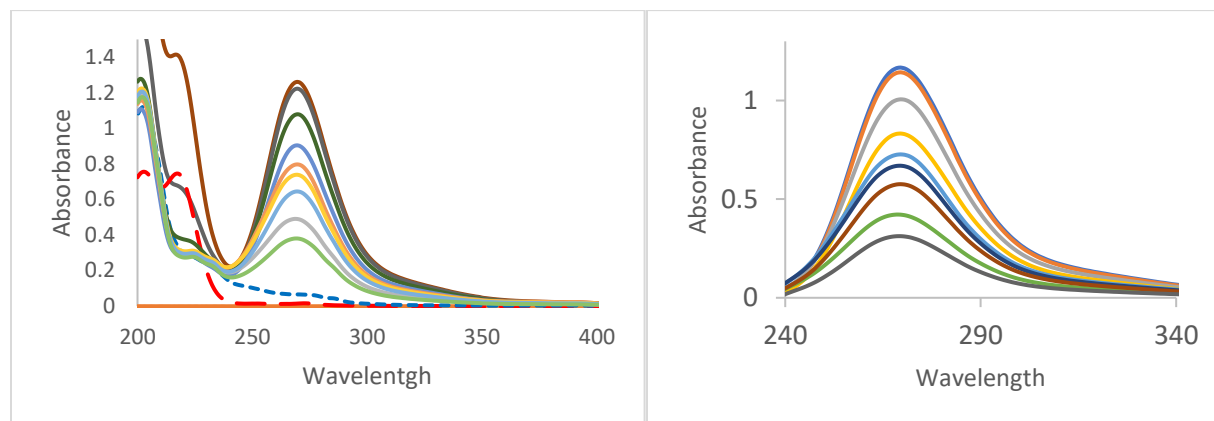


Figure 4: (Left) Uv-Vis spectra of BrSIM-TPABr with individual components as dashed lines, complex shown as solid lines. (Right) Excel graph of BrSAC-TPABr with individual components subtracted out

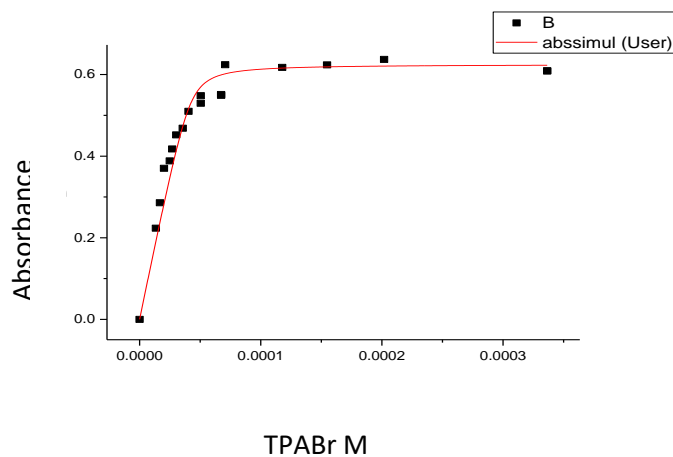


Figure 5: Plot of BrSIM and TPABr concentrations versus absorbance maxima using equation 1.

In this case, using equation 1 as described in the experimental section, this returned an equilibrium constant of  $1 \times 10^3$  and an extinction coefficient of 54 at wavelength 237 nm.

The ISAC and TPABr complex only has one experiment in which data was able to be obtained. This, and many other complexes were run in quick succession after reproducible data was obtained from the two complexes mentioned above. It was decided that getting an accurate picture of more compounds was more important than getting reproducible and accurate final numbers during the time that this experiment was being performed due to the number of complexes that still needed to be studied. Therefore, the following complexes have fewer numbers of experiments that were performed with the specific components than the TPABr and BrSIM and BrSAC complexes described above.

The complex of ISAC and TPABr was studied in a manner similar to what was described in the experimental section and the UV-Vis measurements are shown in Figure 6. The ISAC had a stock concentration of  $2.1 \times 10^{-4}$  M and the TPABr had a stock concentration of  $5.89 \times 10^{-4}$ . The ISAC concentration in complex was held constant at  $5.3 \times 10^{-5}$  M and the TPABr concentration was decreased from  $1.5 \times 10^{-4}$  M to  $7.4 \times 10^{-6}$  M.

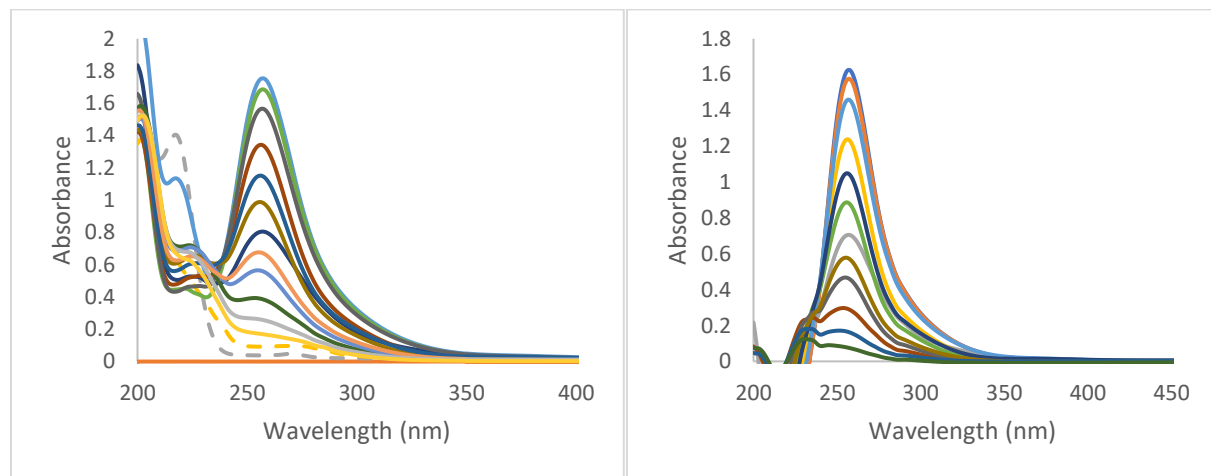


Figure 6: (Left) UV-Vis absorbance spectra of ISAC and TPABr with individual components shown as dashed lines, complex shown as solid lines. (Right) Excel graph spectra of ISAC and TPABr with individual components subtracted out.

This figure shows the complex formation of ISAC:TPABr due to peak formations at wavelength 255 nm with absorbance increasing as the concentration of TPABr increased.

The complex of ISIM and TPABr was studied in a manner consistent with the other bromide acceptors however, the ISIM had a stock concentration of  $2.0 \times 10^{-4}$  M and TPABr had a stock concentration of  $2.0 \times 10^{-4}$ . ISAC concentration in complex was held constant at  $5.0 \times 10^{-5}$  M and TPABr concentration was decreased from  $5.0 \times 10^{-5}$  M to  $1.0 \times 10^{-5}$  M. The results of the Uv-Vis spectrophotometer are shown in Figure 7.

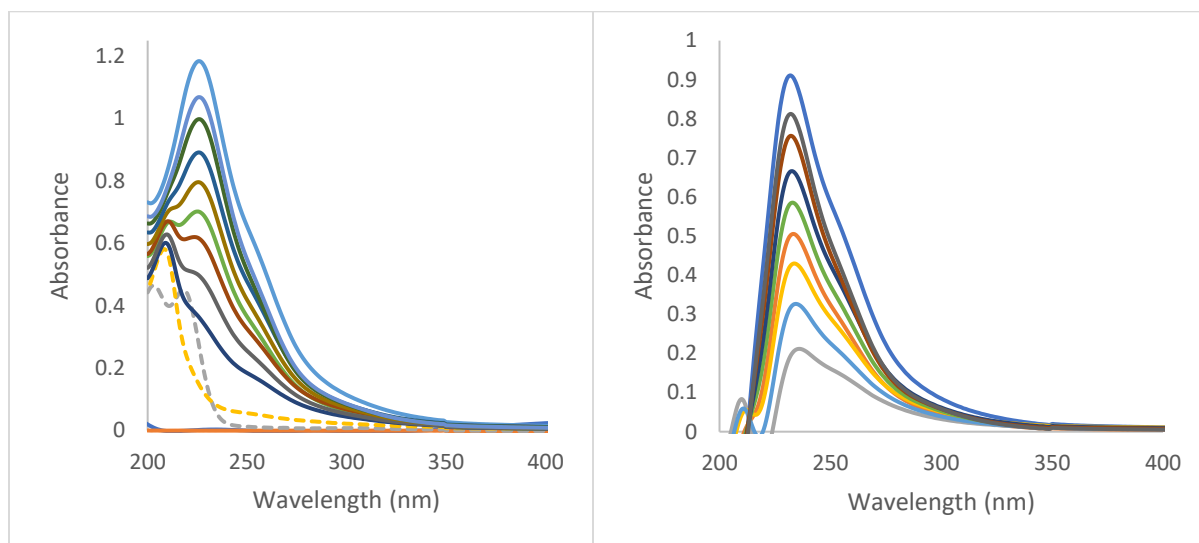


Figure 7. (Left) Uv-Vis spectra of ISIM-TPABr with individual components as dashed lines, complex shown as solid lines. (Right) Excel graph of ISIM-TPABr with individual components subtracted out.

This figure shows the complex formation of ISIM:TPABr due to peak formations at wavelength 232 nm with absorbance increasing as the concentration of TPABr increased.

The complex of ClSAC and TPABr was studied in a manner that was consistent with the bromide acceptors, however the ClSAC had a stock concentration of  $1.7 \times 10^{-4}$  M and the TPABr had a stock concentration of  $2.3 \times 10^{-4}$ . The BrSIM concentration in complex was held constant at  $4.2 \times 10^{-5}$  M and the TPABr concentration was decreased from  $5.8 \times 10^{-5}$  M to  $2.9 \times 10^{-6}$  M. The results of the Uv-Vis spectrophotometer are shown in Figure 8.

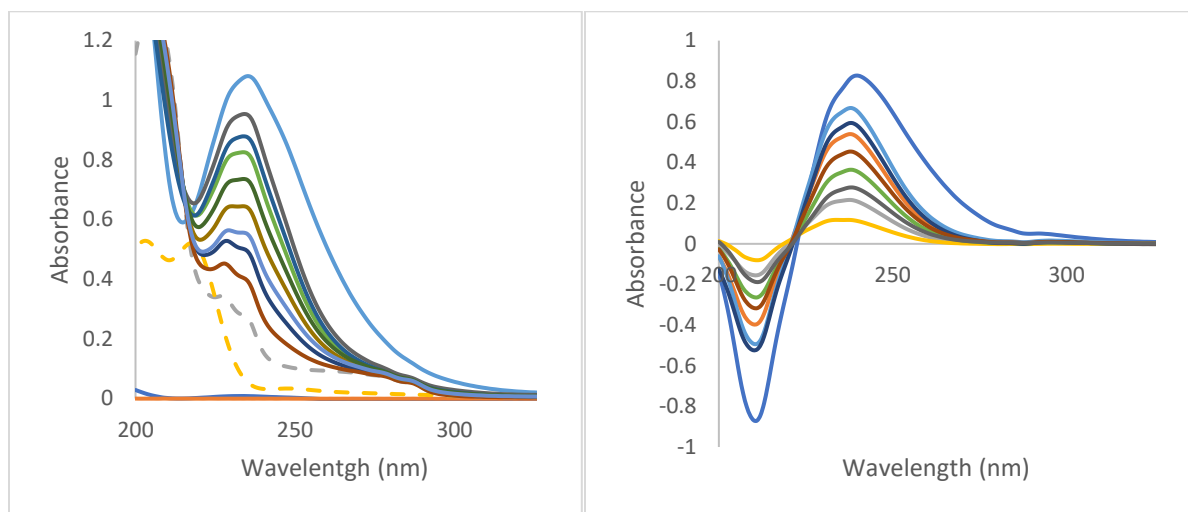


Figure 8: (Left) Uv-Vis spectra of ClSAC-TPABr, left with individual components as dashed lines, complex shown as solid lines. (Right) Uv-Vis spectra of ClSAC-TPABr with individual components subtracted out

This figure shows the complex formation of ClSAC:TPABr due to peak formations at wavelength 245 nm with absorbance increasing as the concentration of TPABr increased.

The complex of ClSIM and TPABr was studied in a manner consistent with the other bromide acceptors, however, the ClSIM had a stock concentration of  $7.5 \times 10^{-3}$  M and the TPABr had a stock concentration of  $1.1 \times 10^{-3}$ . The ClSIM concentration in complex was held constant at  $1.9 \times 10^{-3}$  M and the TPABr concentration was changed from  $2.82 \times 10^{-3}$  M to  $5.6 \times 10^{-5}$  M and the results of the Uv-Vis spectrophotometer are shown in Figure 9.

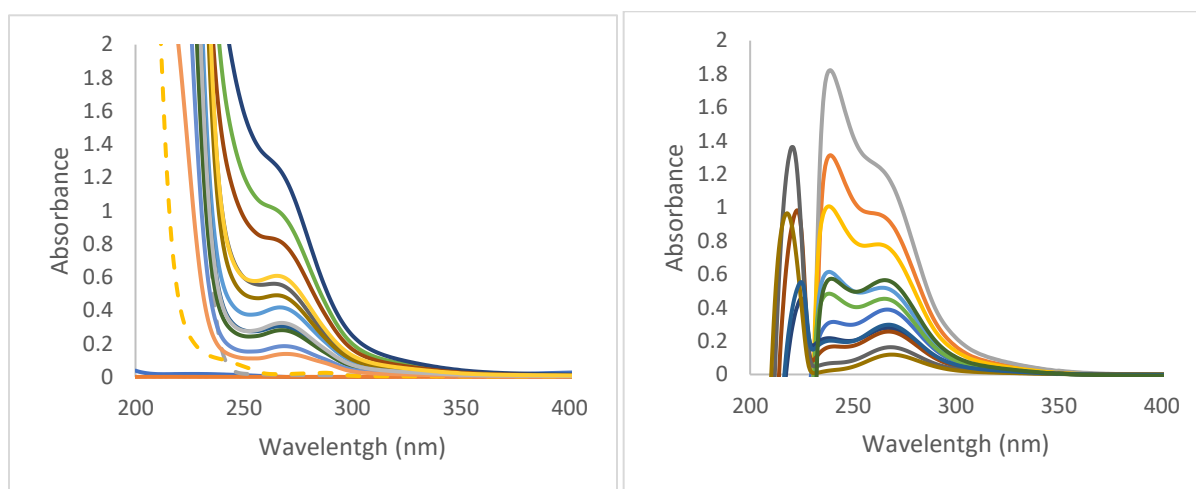


Figure 9: (Left) Uv-Vis spectra of ClSIM-TPABr with individual components as dashed lines, complex shown as solid lines. (Right) Excel graph of ClSIM-TPABr with individual components subtracted out

This figure shows the complex formation of ClSIM:TPABr due to peak formations at wavelength 265 nm with absorbance increasing as the concentration of TPABr increased.



There were fewer measurements done with chloride as the anion due to the humidity of the lab making working with the highly hygroscopic chloride containing salt difficult. Often times the salt would absorb too much moisture from the air while weighing to prepare a solution and so the bromide anion was more readily studied.

The complex of BrSAC and TPACl was one that was studied early on in the research process. This was before the correct ratio was found to have the complex exist as a 1:1 ratio of donor to acceptor and as such the data is unreliable and the graph does not have good separation. This is also why the concentrations of the individual components are much higher than most of the other complexes reported. It was studied similar to the methods described in the later experiments, however the concentrations are far different and as such, much of the series is unable to be viewed properly.

The BrSAC had a stock concentration of  $1.1 \times 10^{-3}$  M and the TPACl had a stock concentration of  $2.0 \times 10^{-2}$ . The BrSAC concentration in complex was held constant at  $5.5 \times 10^{-3}$  M and the TPACl concentration was decreased from  $1.0 \times 10^{-2}$  M to  $2.0 \times 10^{-3}$  M. The results from the Uv-Vis spectrophotometer are shown in Figure 10.

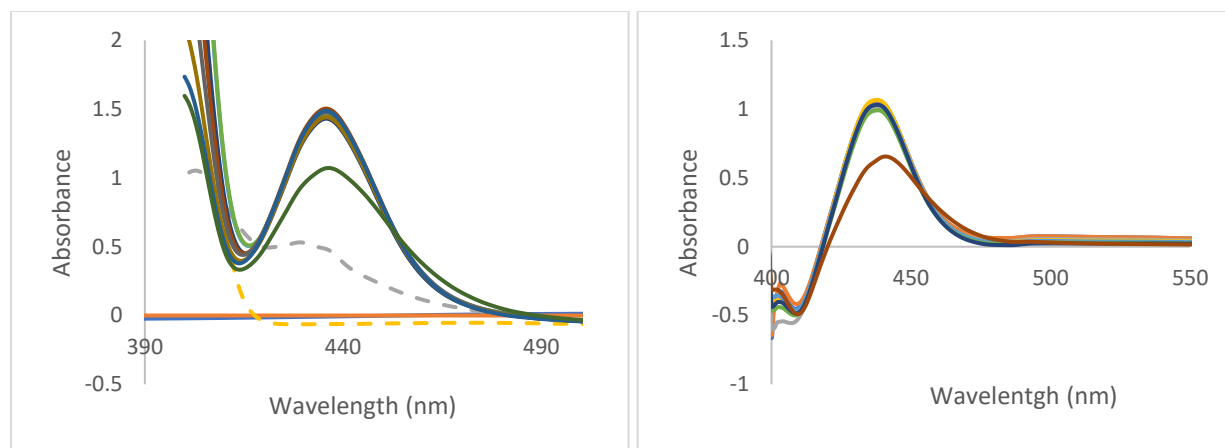


Figure 10: (Left) Uv-Vis spectra of BrSAC-TPACl with individual components as dashed lines, complex shown as solid lines. (Right) Excel graph of BrSAC-TPACl with individual components subtracted out

This figure shows the complex formation of BrSAC:TPACl due to peak formations at wavelength 238 nm with absorbance increasing as the concentration of TPACl increased.

The ClSAC and TPACl complex was the first chloride complex that was revisited after the proper ratio was found. This was significantly later into the research process and as such presents data that looks similar to the bromide complexes that were seen earlier.

The complex of ClSAC and TPACl was studied in a manner consistent with the description in the experimental section. The Uv-Vis measurements are shown in Figure 11. The ClSAC had a stock concentration of  $5.3 \times 10^{-3}$  M and the TPACl had a stock concentration of  $6.8 \times 10^{-2}$ . The ClSAC concentration in complex was held constant at  $2.7 \times 10^{-3}$  M and the TPACl concentration was decreased from  $3.4 \times 10^{-2}$  M to  $4.5 \times 10^{-3}$  M.

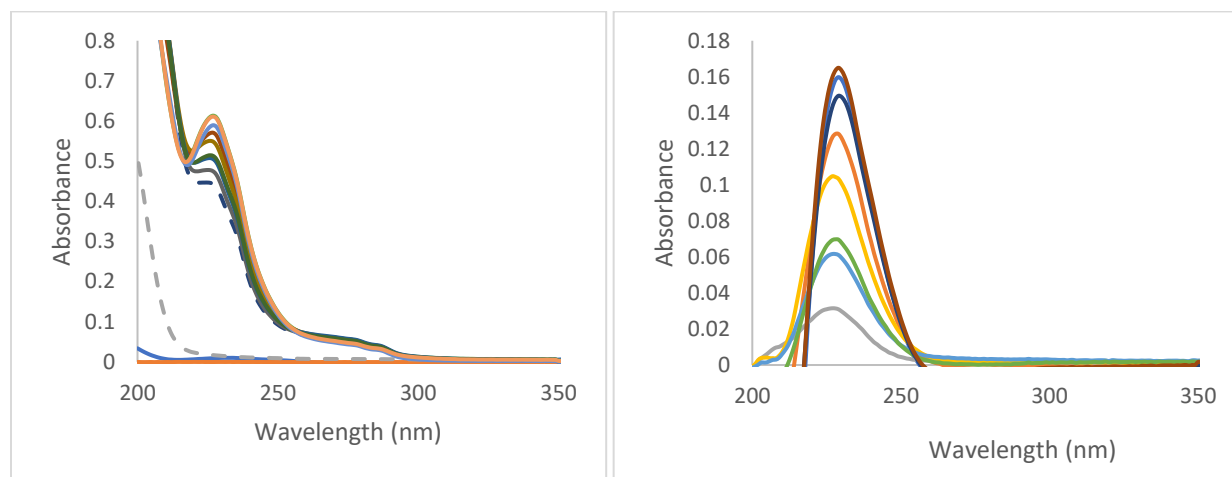


Figure 11: (Left) Uv-Vis spectra of ClSAC-TPACl with individual components as dashed lines, complex shown as solid lines. (Right) Uv-Vis spectra of ClSAC-TPACl with individual components subtracted out

This figure shows the complex formation of ClSIM:TPACl due to peak formations at wavelength 228 nm with absorbance increasing as the concentration of TPACl increased.

The complex of ISAC and TPACl was studied in a manner consistent with the chloride acceptors, and the Uv-Vis results are shown in Figure 12. However, the ISAC had a stock concentration of  $1.9 \times 10^{-4}$  M and the TPACl had a stock concentration of  $6.4 \times 10^{-4}$ . The ClSIM concentration in complex was held constant at  $4.6 \times 10^{-5}$  M and the TPACl concentration was changed from  $1.6 \times 10^{-4}$  M to  $6.4 \times 10^{-6}$  M.

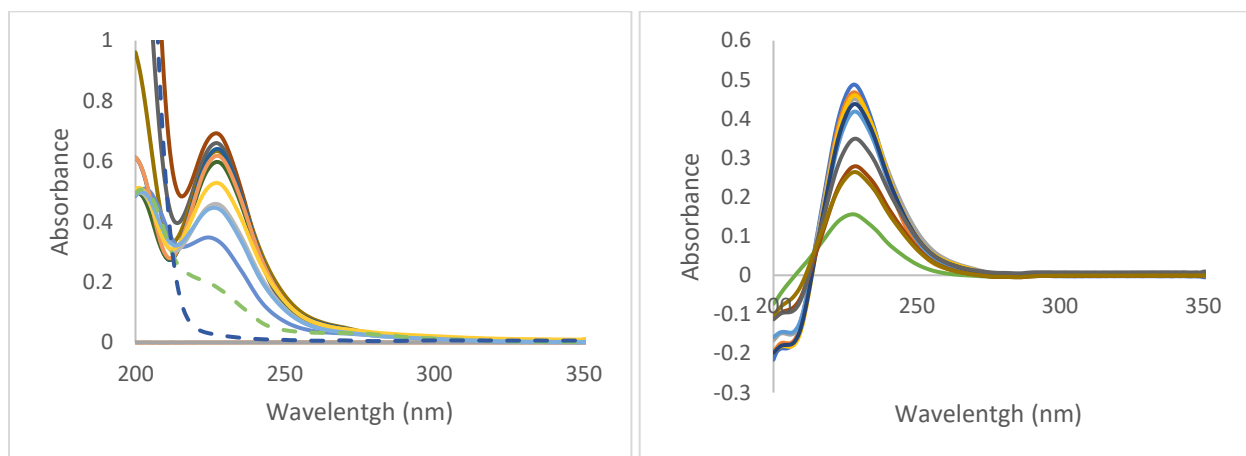


Figure 12: (Left) Uv-Vis spectra of ISAC-TPACl with individual components as dashed lines, complex shown as solid lines. (Right) Excel graph of ISAC-TPACl with individual components subtracted out

This figure shows the complex formation of ISAC:TPACl due to peak formations at wavelength 228 nm with absorbance increasing as the concentration of TPACl increased.

The complex of ClSIM and TPACl was studied in a manner consistent with the chloride acceptors, and the results from the Uv-Vis spectrophotometer are shown in Figure 13. However, the ClSIM had a stock concentration of  $1.2 \times 10^{-3}$  M and the TPACl had a stock concentration of  $1.2 \times 10^{-3}$ . The ClSIM concentration in complex was held constant at  $3.1 \times 10^{-4}$  M and the TPACl concentration was changed from  $3.0 \times 10^{-4}$  M to  $6.0 \times 10^{-6}$  M.

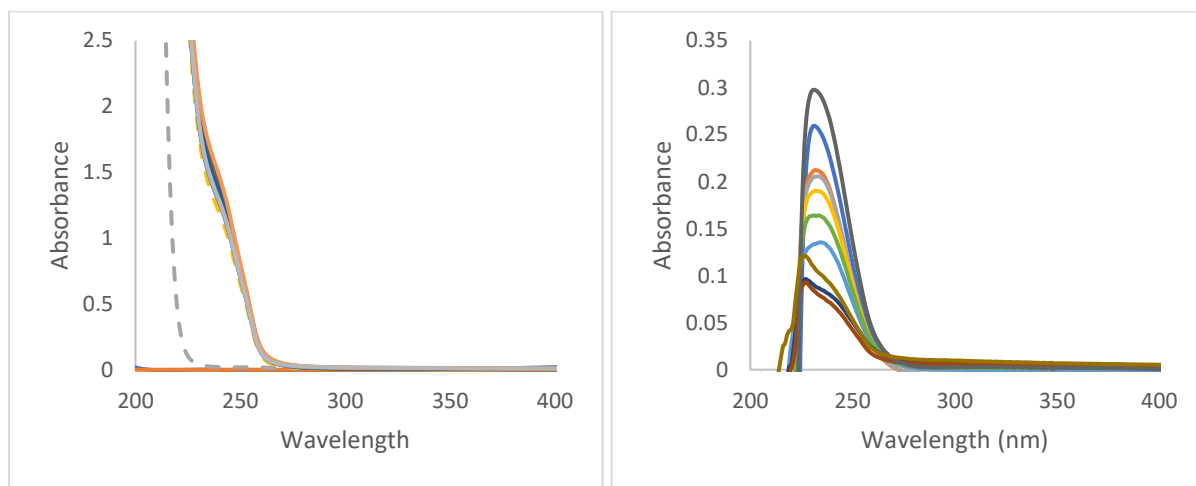


Figure 13: (Left) Uv-Vis spectra of ClSIM-TPACl. left with individual components as dashed lines, complex shown as solid lines. (Right) Excel graph of ClSIM-TPACl with individual components subtracted out

This figure shows the complex formation of ClSIM:TPACl due to peak formations at wavelength 265 nm with absorbance increasing as the concentration of TPACl increased.

Finally, the complex of ISIM and TPACl was studied in a manner consistent with the chloride acceptors, and the results from the Uv-Vis spectrophotometer are shown in Figure 14. However, the ISIM had a stock concentration of  $2.0 \times 10^{-3}$  M and the TPACl had a stock concentration of  $2.0 \times 10^{-3}$ . The ISIM concentration in complex was held constant at  $5.0 \times 10^{-5}$  M and the TPACl concentration was decreased from  $5.0 \times 10^{-5}$  M to  $7.9 \times 10^{-6}$ .

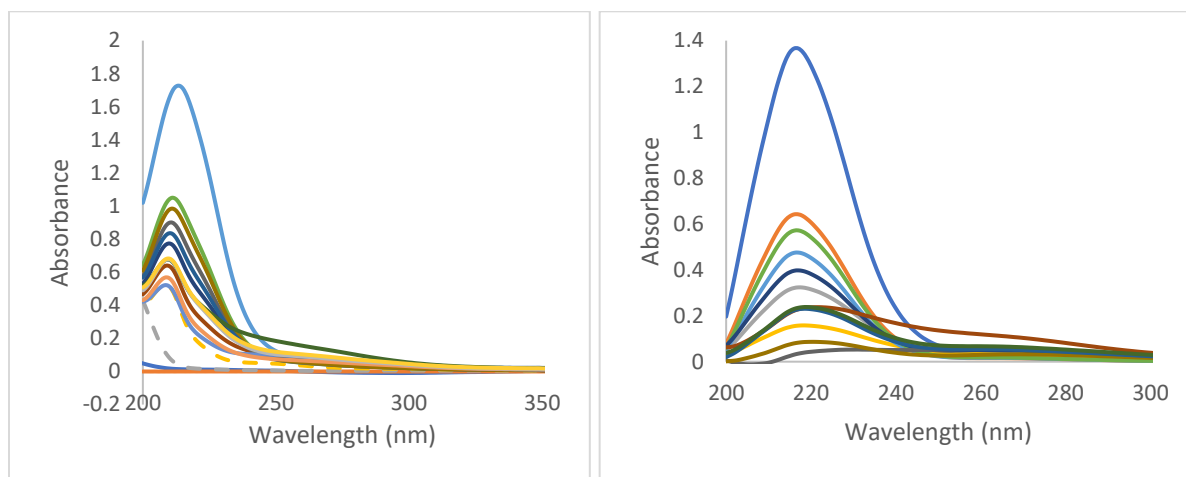


Figure 14: (Left) Uv-Vis spectra of ISIM-TPACl with individual components as dashed lines, complex shown as solid lines. (Right) Uv-Vis spectra of ISIM-TPACl with individual components subtracted out

This figure shows the complex formation of ISIM:TPACl due to peak formations at wavelength 232 nm with absorbance increasing as the concentration of TPACl increased.

The  $\epsilon$  and  $K_{eq}$  values were obtained from a regression analysis and equation 1 in the experimental section. Table 1 includes values from the bromide anion and Table 2 includes the values from the chloride anion.

Table 1: Wavelength at maximum absorption, extinction coefficient and equilibrium constant for bromide anion

	$\lambda_{max}$ , nm	$\epsilon$ , $M^{-1} cm^{-1}$	$K_{eq}$ , $M^{-1}$
BrSAC	270	$5.1 \times 10^4$	$1.1 \times 10^5$
CISAC	242	$1.1 \times 10^4$	$6.0 \times 10^6$
ISAC	255	$1.6 \times 10^4$	$1.0 \times 10^6$
BrSIM	237	54	$1.0 \times 10^3$
CISIM	265	$2.1 \times 10^3$	$1.4 \times 10^2$
ISIM	232	$3.6 \times 10^5$	$4.0 \times 10^3$

Table 2: Wavelength at maximum absorption, extinction coefficient and equilibrium constant for chloride anion

	$\lambda_{\text{max}}$ nm	$\epsilon$ , $\text{M}^{-1} \text{cm}^{-1}$	$K_{\text{eq}}$ , $\text{M}^{-1}$
BrSAC	238	$5.1 \times 10^4$	$1.1 \times 10^5$
CISAC	228	$4.3 \times 10^3$	$5.8 \times 10^5$
ISAC	228	-	-
BrSIM	230	28	$1.0 \times 10^3$
CISIM	265	74	293
ISIM	232	$1.4 \times 10^6$	$6.2 \times 10^3$

The data in these tables show very high equilibrium constants and extinction coefficients compared to other similarly bonded complexes. With  $K_{\text{eq}}$  values ranging between 293 to  $6 \times 10^6$  these are on the order of 20-60000 times higher than other complexes.

There also does not seem to be any consistent wavelength that these peaks appear at between either the donors or acceptors. There are only two halogen bond donors that have complexes that absorb at the same wavelength between the two acceptors that were studied. Those donors being CISIM and ISIM. The acceptors that ended with the same absorbance values was  $\text{Cl}^-$  in the case



of ISAC and ClSAC. Other than that, there appears to be no discernable pattern between these halogen bond acceptors and halogen bond donors when it comes to determining the wavelength that the complexes form at.

Iodide complex measurements did not have  $K_{eq}$  or  $\epsilon$  measured in this experiment because when it was mixed with a halogen donor, it would form  $I_3^-$ . This formation of  $I_3^-$  means that it did not form a halogen bonded complex, and instead underwent a redox reaction with the halogen containing imide or saccharine. This was confirmed with the UV-Vis measurements by observing a large band around 360nm which is indicative of the formation of  $I_3^-$ . Additionally, the iodide anion was largely time dependent in its measurements. This means that it could not be measured in the same way that the other complexes were and thus were not included in the results of this experiment.

## Section II- Time dependent complexes

BrSIM and TPAI was the only system that currently observed the time dependency of the iodide anion. Other experiments were run with variable concentrations of the iodide anion, but the thermodynamic properties of the data were inconsistent and not reliable. It was noted that the system may be time dependent early on, but it was not shown through an actual experiment until much later in the research process as other anions were studied.

The complex of BrSIM and TPAI was studied by a method similar to those described in the experimental section with the key differences noted here. The Uv-Vis spectrophotometer measurements are shown in Figure 15. The BrSIM had a stock concentration of  $2.4 \times 10^{-4}$  M and the TPAI had a stock concentration of  $5.0 \times 10^{-4}$ . The BrSIM concentration in solution was  $1.2 \times 10^{-4}$  and the TPAI concentration in solution was held at  $2.5 \times 10^{-4}$  and not decreased. The solution was allowed to react over one hour as Uv-Vis spectra were taken between 1-5 minutes apart in a 1cm cuvette.

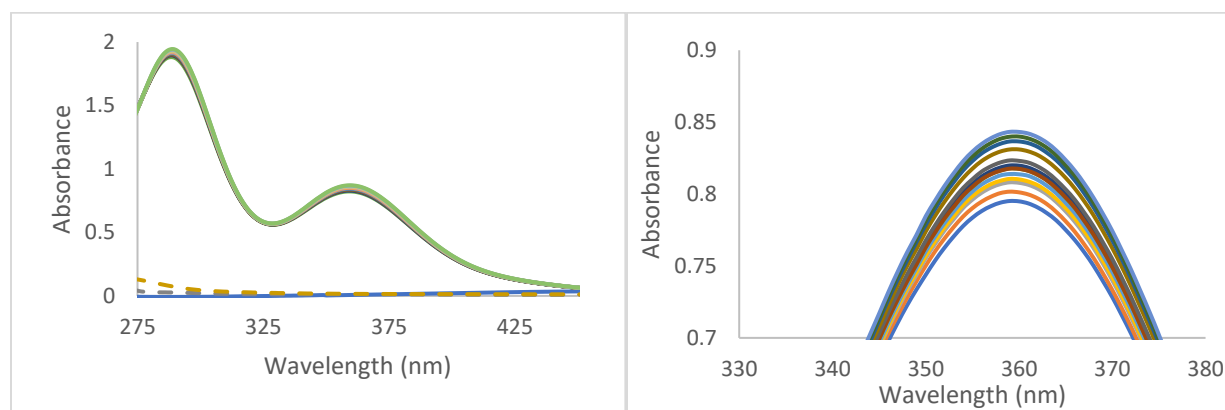


Figure 15: (Left) Uv-Vis spectra of BrSIM-TPAI with individual components as dashed lines, complex shown as solid lines. (Right) Excel graph of BrSIM-TPAI with individual components subtracted out

In this complex, the absorbance values increased at 359 nm as time progressed. This indicates the formation of  $I_3^-$  rather than a halogen bond which were primarily in the 230-270 nm range.

The phthalimide compounds were recent additions to the halogen donor organic attachments, and as such it was unknown what to expect with their complexes. It appears that the complexes were highly time dependent no matter the anion that was attached, when previously it had only been iodide that was time dependent. It also showed time dependence with different halogens acting as the donors.

The complex of BrPIM and TPABr was studied over the course of 1 hour in a 1cm cuvette. Each trial was between 1-7 minutes apart with the time increasing between measurements as the experiment progressed. The Uv-Vis spectra are shown in Figure 16. The BrPIM had a stock concentration of  $9.0 \times 10^{-4}$  M and the TPABr had a stock concentration of  $1.1 \times 10^{-3}$ . The BrPIM concentration in solution was  $2.3 \times 10^{-4}$  and the TPABr concentration in solution was held at  $2.4 \times 10^{-4}$ .

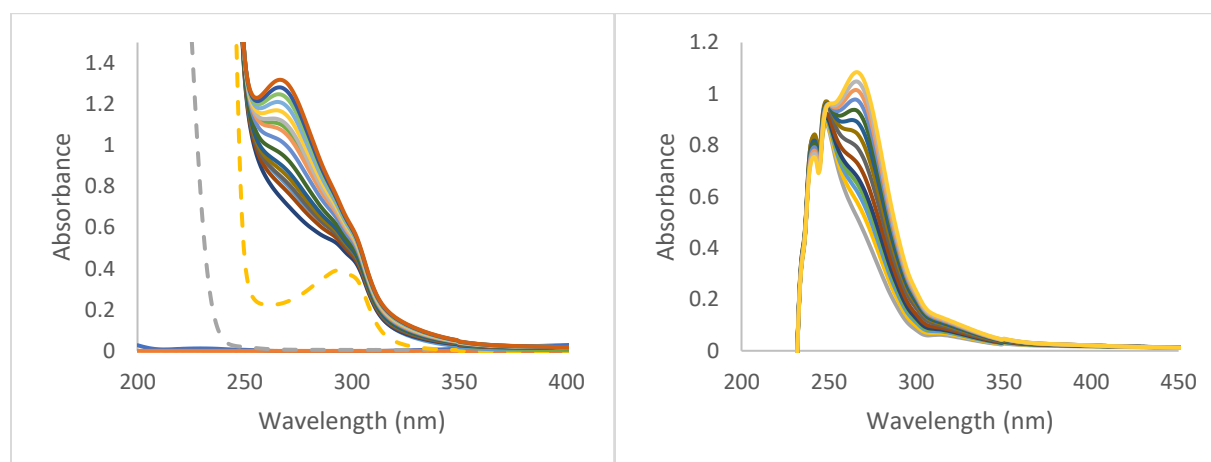


Figure 16: (Left) Uv-Vis spectra of BrPIM-TPABr with individual components as dashed lines, complex shown as solid lines. (Right) Excel graph of BrPIM-TPABr with individual components subtracted out

The absorbance of this spectra and the wavelength that the peak absorbance appeared at increased as time progressed in this complex. The wavelength at the maximum absorbance peak was at 266 nm.

The complex of CIPIM and TPABr was studied in a manner consistent with that of the other PIM donors. However, the CIPIM had a stock concentration of  $1.2 \times 10^{-3}$  M and the TPABr had a stock concentration of  $9.2 \times 10^{-4}$ . The CIPIM concentration in solution was  $6.0 \times 10^{-4}$  and the TPABr concentration in solution was held at  $4.6 \times 10^{-4}$ . The Uv-Vis spectra are shown in Figure 17.

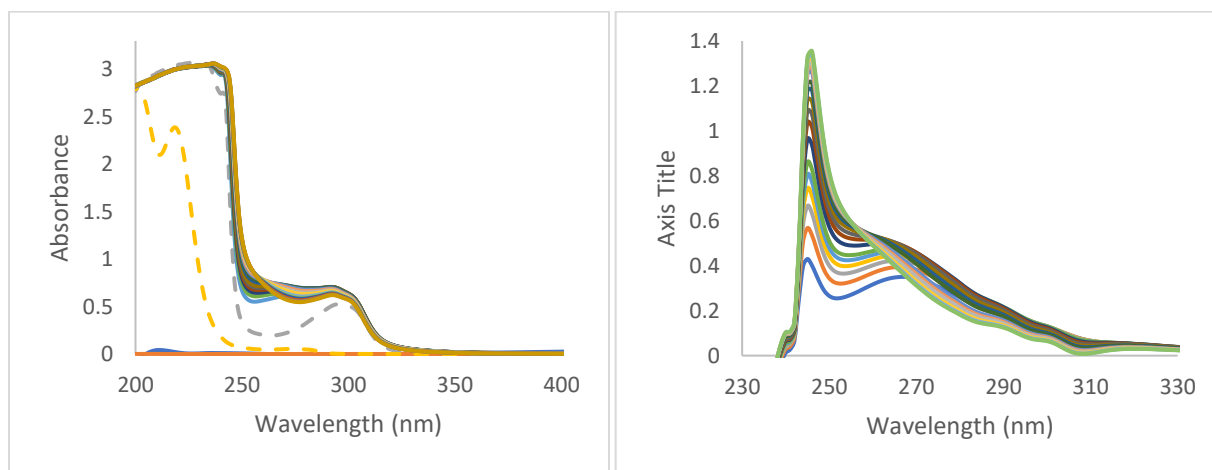


Figure 17: (Left) Uv-Vis spectra of CIPIM-TPABr with individual components as dashed lines, complex shown as solid lines. (Right) Excel graph of CIPIM-TPABr with individual components subtracted out

The absorbance of this spectra and the wavelength that the peak absorbance appeared at increased as time progressed in this complex. The wavelength at the maximum absorbance was at 246 nm.

The complex of CIPIM and TPACl was studied in a manner consistent with the other PIM donors. However, the CIPIM had a stock concentration of  $1.2 \times 10^{-3}$  M and the TPABr had a stock concentration of  $5.1 \times 10^{-2}$ . The CIPIM concentration in solution was  $6.0 \times 10^{-4}$  and the TPABr concentration in solution was held at  $2.6 \times 10^{-2}$ . The Uv-Vis spectra are shown in Figure 18.

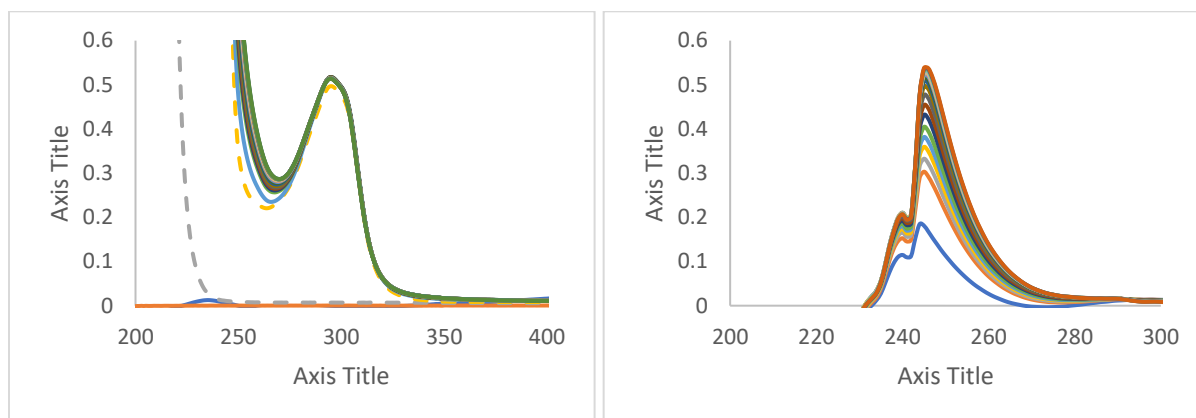


Figure 18: (Left) Uv-Vis spectra of CIPIM-TPACl with individual components as dashed lines, complex shown as solid lines. (Right) Excel graph of CIPIM-TPACl with individual components subtracted out

The absorbance of this spectra and the wavelength that the maximum absorbance appeared at increased as time progressed. The wavelength at the maximum absorbance was at 245 nm.

The complex of BrPIM and TPACl was in a manner consistent with the other PIM donors. However, the BrPIM had a stock concentration of  $9.8 \times 10^{-4}$  M and the TPACl had a stock concentration of  $8.9 \times 10^{-4}$ . The BrPIM concentration in solution was  $4.9 \times 10^{-4}$  and the TPACl concentration in solution was held at  $4.5 \times 10^{-4}$ . The Uv-Vis spectra are shown in Figure 19.

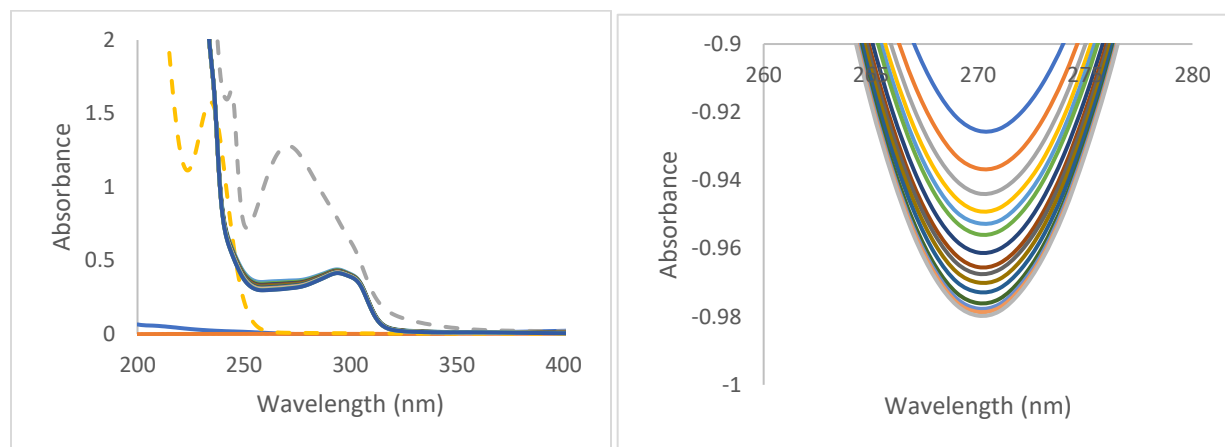


Figure 19: (Left) Uv-Vis spectra of BrPIM-TPACl with individual components as dashed lines, complex shown as solid lines. (Right) Uv-Vis spectra of BrPIM-TPACl with individual components subtracted out

The absorbance of this complex decreased as time progressed. This is unusual for all of the complexes studied as the complex absorbed below the individual component whereas in all other cases the complex absorbed higher than the individual component of the complexes. And the wavelength that corresponds to the absorbance minimum in this case appeared at 270. The wavelength that the complex absorbed at did not change in this experiment like it did in the others, further separating it from the other similar complexes.

Further analysis must be done as far as time dependency is concerned as the current method for calculation of  $K$  and  $\epsilon$  do not account for time as a variable in the complex.

## Conclusion

From this data it can be clearly seen that strong halogen bonding occurs in many of the complexes studied. This is noted through the change in their absorbance bands after mixing and a shortening. The strength of the bonding that was measured was much higher than that of traditionally bonded complexes. Usually these complexes have  $K_{eq}$  values ranging from 1-10 and 10 is considered to be a rather strongly bonded complex. From these measurements, the lowest bonding constant is approximately 3x higher than what is considered a strongly bonded complex. From this it can be determined that strong halogen bonding has occurred and that it is much stronger than what is considered to be traditionally bonded complexes.

Iodide as a halogen bond acceptor was not measured in this experiment due to its time dependent nature not allowing for the calculation of the thermodynamic constants required for this research.

Finally, pthlalimide measurements were also seen to be time dependent no matter the anion attached. This warrants further study as to why these complexes are highly time dependent when the other similarly structured organic molecules show no time dependency.

## References

1. Cavallo, G.; Metrangolo, P.; Milani, R.; Pilati, T.; Priimagi, A.; Resnati, G.; and Terraneo, G. The Halogen Bond Chem. Rev., 2016, 16, 2478
2. Politzer, P.; Murray, J.; and Clark, T. Halogen bonding and other  $\sigma$ -hole interactions: a perspective. Phys.Chem. Chem. Phys. 2010, 12, 7748. (b) P. Politzer, J. Murray and T. Clark, Phys.Chem. Chem. Phys. 2013, 15, 11178.
3. Rosoka, S.; Watson, B.; Grounds, O.; Borley W. Resolving the Halogen vs. Hydrogen Bonding Dichotomy in Solutions: Intermolecular Complexes Of Trihalomethanes With Halide and Pseudohalide. Anions Phys. Chem. Chem. Phys., 2018, 20, 21999.
4. Rosokha, S.; and Kumar, A. Anion- $\Pi$  Interaction in Metal-Organic Networks Formed by Metal Halides and Tetracyanopyrazine. J. Mol. Struct., 2017, 1138, 129.
5. Legon A. Angew. Prereactive Complexes of Dihalogens. XY with Lewis Bases B in the Gas Phase: A Systematic Case for the Halogen Analogue B  $\cdots$  XY of the Hydrogen Bond B  $\cdots$  HX. Chem. Int. Ed 1999, 38, 2686–2714.